Epistasis and cryptic QTL identified using modified bulk segregant analysis of copper resistance in budding yeast

Cassandra Buzby[1,2], Yevgeniy Plavskin[1,2], Federica M.O. Sartori[1,2,3], Qiange Tong[1,2], Janessa K. Vail[1,2], Mark L. Siegal[1,2*]

[1] Department of Biology, New York University, New York, NY, USA

[2] Center for Genomics and Systems Biology, New York University, New York, NY, USA

[3] Current affiliation: Department of Oncological Sciences, Mount Sinai, New York, NY, USA

* Corresponding author

E-mail: mark.siegal@nyu.edu (MLS)

Abstract

The contributions of genetic interactions to natural trait variation are challenging to estimate experimentally, as current approaches for detecting epistasis are often underpowered. Powerful mapping approaches such as bulk segregant analysis, wherein individuals with extreme phenotypes are pooled for genotyping, obscure epistasis by averaging over genotype combinations. To accurately characterize and quantify epistasis underlying natural trait variation, we have engineered strains of the budding yeast *Saccharomyces cerevisiae* to enable crosses where one parent's chromosome is fixed while the rest of the chromosomes segregate. These crosses allow us to use bulk segregant analysis to identify quantitative trait loci (QTL) whose effects depend on alleles on the fixed parental chromosome, indicating a genetic interaction with that chromosome. Our method, which we term epic-QTL (for *epi*static-with-*c*hromosome *QTL*) analysis, can thus identify interaction loci with high statistical power. Here we perform epic-QTL analysis of copper resistance with chromosome I or VIII fixed in a cross between divergent naturally derived strains. We find seven loci that interact significantly with chromosome VIII and none that interact with chromosome I, the smallest of the 16 budding yeast chromosomes. Each of the seven interactions alters the magnitude, rather than the direction, of an additive QTL effect. We also show that fixation of one source of variation — in this case chromosome VIII, which contains the large-effect QTL mapping to *CUP1* — increases power to detect the contributions of other loci to trait differences.

Author Summary

Most traits of interest that vary in populations are determined by multiple genetic factors, as well as by environmental variation and random chance. These influences may combine in complicated ways, for example when the effect of one genetic variant depends on genetic variants elsewhere in the genome. Such dependencies are difficult to identify and characterize because testing many possible combinations of influences reduces statistical power. We address this challenge by combining bulk segregant analysis, a robust method for detecting effects of individual genetic variants averaged across genetic backgrounds, with chromosome fixation in budding yeast. This approach allows us to detect gene-variant effects that depend on the fixed chromosome with statistical power comparable to that achieved when detecting background-independent effects. Applying the approach to copper sulfate resistance, we identify and characterize interaction effects and, by removing one source of variation (a single yeast chromosome), improve detection of background-independent effects as well.

Introduction

Predicting phenotype from genotype is a central goal of genetics research, yet even with great advances in sequencing technology and experimental scale, accurate characterization of how genetic differences translate into trait differences remains elusive. Many genetic influences are subtle, and most traits of interest that vary in populations are determined by multiple genetic factors, as well as by environmental variation and random chance [1–4]. Moreover, these influences may combine in

68 complicated ways, for example in the form of gene-by-gene (epistatic) or gene-by-
69 environment interactions [5–7].

70 Epistasis is particularly challenging to detect in standard quantitative-genetic
71 analyses because the number of possible interaction effects vastly exceeds the number
72 of single-locus (additive) effects, leading to very low statistical power to detect the
73 interactions [5]. Standard analyses fit additive effects before interaction effects, which
74 can lead to the mistaken inference that epistasis is less salient than it actually is [8,9]. If
75 interacting alleles are rare in a mapping population, under-detection of epistasis is even
76 more severe. Failure to detect epistasis in turn compromises accurate prediction of an
77 individual's phenotype from genotype, even when an additive model appears to fit well
78 [8–10].

79 The distribution of types of epistatic effects influences both detection of loci with
80 effects on traits and evolutionary trajectories [11–13]. Magnitude epistasis changes the
81 size of an allele's effect without changing its direction (beneficial vs. detrimental),
82 whereas sign epistasis changes the direction. Sign epistasis gives rise to peaks and
83 valleys in fitness landscapes and can alter the order of mutations that increase fitness
84 [11]. Models of distribution and patterns of these effects have been postulated, with two
85 extremes being global epistasis and idiosyncratic epistasis. Global epistasis indicates
86 underlying predictability of the effects of individual alleles, perhaps based on a latent
87 phenotype such as protein stability or physiological health [14,15]. Idiosyncratic
88 epistasis, by contrast, refers to unpredictable allele effects that ultimately depend on
89 details of particular alleles [16,17]. Data on the relative prevalences of magnitude and
90 sign epistasis, which are currently lacking, would inform which model of epistasis

91 patterns is more suitable, which in turn will inform models of the evolution of complex
92 traits.

93 An ideal method for identifying and characterizing epistatic contributions to trait
94 variation would have equal (and high) statistical power to detect additive and interaction
95 effects. Experimental designs with extremely large sample sizes are now common [18–
96 22], but the most powerful of these favor (or exclusively detect) additive effects. One
97 such experimental design is bulk segregant analysis (BSA). In a typical BSA
98 experiment, many progeny are produced from a cross between divergent parental
99 genotypes, progeny with extreme values of a trait of interest are pooled, and high-
100 coverage genome sequencing is used to detect loci at which the allele frequency in the
101 selected bulk deviates significantly from the allele frequency in an unselected (or
102 oppositely selected) bulk [18,23]. Although BSA benefits from sampling many
103 individuals — over 10 million in some cases [18] — it cannot detect genetic interaction
104 effects because pooled sequencing results in an estimate of the effect of any one locus
105 that is the average across all genotypes at other loci.

106 Genotyping and phenotyping individuals rather than pools avoids the averaging
107 issue, but suffers from the problem that potential pairwise interactions far outnumber
108 additive effects of single loci, resulting in greatly reduced statistical power. Two recent
109 attempts to detect epistasis using very large sample sizes illustrate this challenge. One
110 study, which genotyped ~200,000 diploid progeny of a yeast cross, identified numerous
111 interaction effects, but found a strong positive correlation between the additive effect of
112 a locus and the number of pairwise interactions it participates in [22]. This correlation
113 could reflect the true distribution of epistatic effects or an influence of additive-effect size

114 on detectability of interactions [22]. Another study genotyped ~100,000 haploid
115 segregants but to maximize power tested only interactions between pairs of additive-
116 effect QTL [21]. This study found evidence of epistatic effects, but found the additive-
117 plus-pairwise model to have only modest predictive power for the phenotypes of
118 reconstructed genotypes, suggesting that effects remain undetected [21]. Another
119 recent study did not genotype large numbers of segregants, but instead engineered
120 naturally occurring gene variants into four divergent yeast strains to detect genetic
121 background-dependent effects on growth. This study found a substantial fraction of
122 variants to have background-dependent effects, but was limited to variants in and
123 around 103 genes previously shown to be interaction hubs in genome-wide double-
124 mutant screens [24,25]. The results of these studies suggest that unbiased approaches
125 are needed that equalize the power to detect additive and epistatic effects.
126 To identify and characterize genetic interactions with comparable statistical
127 power to that of additive effects, we combine chromosome substitution with BSA in the
128 genetically tractable budding yeast, *Saccharomyces cerevisiae*. We call this method
129 epic-QTL (for *epi*static-with-*c*hromosome *QTL*) analysis. To perform epic-QTL, we cross
130 two divergent natural isolates of *S. cerevisiae*, but before generating segregating F2
131 progeny from the resulting F1 diploid, we first eliminate one chromosome from one
132 parent, fixing the remaining homologous chromosome. The result is that all surviving F2
133 haploids contain identical copies of one chromosome, but have unique combinations of
134 the two parents' alleles on all other chromosomes. We also perform the reciprocal
135 cross, in which the other parent's chromosome is fixed. We then grow the haploid
136 progeny in selective or non-selective conditions. Here, we use the presence or absence

137 of copper (II) sulfate ($CuSO_4$) as a selective condition, with the presence of copper and
138 subsequent oxidative stress selecting for individuals with alleles that promote survival in
139 this environment. Standard BSA would compare the allele frequencies in bulks grown in
140 the presence or absence of copper to identify additive QTL for the trait of copper
141 resistance. In epic-QTL, there are four bulks rather than two. By comparing the QTL
142 identified in the crosses with the reciprocal fixed chromosomes, we can identify loci
143 whose effects differ between genetic backgrounds. The loci that are dependent on
144 parental-chromosome background for their effect are thus epistatic with that fixed
145 chromosome and are detected with statistical power usually only afforded to additive
146 effects. In practice, this comparison is done by including a parental-chromosome (or
147 genetic-background) term in a logistic-regression model that is fit to the data from all
148 four bulks simultaneously. An additional benefit of chromosome substitution is an
149 increase in power for detection of additive effects by removing a source of variance in a
150 population. With only one cross, the fixation of a chromosome containing a major QTL
151 allows the remaining segregating sites to exert greater influence over membership in
152 the selected bulk.

153 Using epic-QTL we can determine where QTL that interact with each fixed
154 chromosome lie relative to where additive QTL lie, and how prevalent interactions are
155 for a given trait, in this case copper sulfate resistance. We focus on copper sulfate for
156 three reasons: 1) its extensive use in prior *S. cerevisiae* studies, allowing comparison
157 with previous results; 2) the potential for unexplained heritability, in that copper
158 resistance shows a large gap in broad and narrow sense heritability compared to other
159 traits [4]; and 3) its ecological and physiological relevance [26–28]. In addition, one

160 major interaction hub identified by Matsui *et al.* was *CUP1* on chromosome VIII, which is
161 a major driver of copper resistance, and thus a perfect candidate for chromosome
162 fixation [22]. We fixed chromosomes I or VIII in a cross between strains derived from an
163 oak tree or from a wine barrel, which differ on average at 1 in 200 base pairs [29]. The
164 variants in these strains reflect natural genetic diversity, offering insights into genetic
165 interactions that might occur within populations. We demonstrate that this method can
166 be used to remove sources of trait variation to reveal additive QTL otherwise
167 undetected at this experimental scale, as well as to identify interaction QTL with high
168 statistical power. We find that these interactions often occur within significant additive
169 QTL peaks, providing evidence of a lack of pervasive sign epistasis.

170

171 Results

172

173 Implementation of epic-QTL for copper resistance

174 Our method to identify QTL interacting with a fixed chromosome, or epic-QTL,
175 combines chromosome substitution with BSA in a cross of two parental yeast strains.
176 For the parental strains we used divergent natural isolates of *S. cerevisiae*: NCYC3631
177 and NCYC3591 (hereafter “Oak” and “Wine”, respectively). Before crossing the two
178 strains, we engineered one strain of each parent to contain the inducible *GAL1*
179 promoter (*pGAL1*) adjacent to the centromere of one chromosome. Inducing a high
180 level of transcription through the centromere destabilizes the kinetochore, resulting in
181 missegregation of the chromosome during mitosis so that a strain with only the

182 homologous chromosome remaining can be isolated [30]. By this method, we fixed
183 chromosome I in each background (Fig 1A) and, separately, chromosome VIII in each
184 background (Fig 1B). We then mated the Wine *pGAL1* strain with the Oak non-*pGAL1*
185 strain (Fig 1C), and vice versa, to produce diploids with reciprocal conditional
186 chromosomes. Each diploid strain was then plated on galactose to induce *pGAL1*. After
187 re-plating colonies from the galactose-containing media to ensure clonality, individual
188 colonies were checked by Sanger sequencing at biallelic regions to confirm loss of the
189 conditional chromosome. Each of these aneuploid (2N–1) strains was then sporulated
190 to produce an F2 population of haploid segregants fixed for a single parent's
191 chromosome (Fig 1C), which could then be used for BSA (Fig 1D).
192
193 **Fig 1. Insertion of *GAL1* promoter allows for fixed chromosomes.** (A–B) Matings to
194 produce reciprocal diploids with single conditional chromosomes for chromosome I (A)
195 and chromosome VIII (B). (C) Induction of the *GAL1* promoter adjacent to the
196 centromere destabilizes the chromosome's kinetochore, leading to loss of that
197 chromosome in diploids and fixation of the homologous chromosome in F2 haploid
198 progeny. One representative cross of the four (Oak I) is shown. (D) BSA experiment for
199 interactions with chromosome I, allowing detection of additive effects by comparison of
200 selected (blue) and unselected (white) bulks and of interactions with chromosome I
201 background (orange or purple). One representative haploid segregant is shown beneath
202 each bulk's flask.
203

204 Before proceeding to BSA, we demonstrated that the Oak and Wine parental
205 strains, which have been shown to differ phenotypically in multiple traits [31,32], differ in
206 the phenotype of copper sulfate resistance. We grew populations of haploids of each
207 parental strain in an array of doses of $CuSO_4$ in rich media (YPD), and compared the
208 cell counts of each population to a control of the same seed culture. The Wine haploid
209 strain showed higher resistance to $CuSO_4$, surviving at almost double the percentage at
210 which the Oak haploid strain survived in mid-range doses of $CuSO_4$ (S1 Fig).
211 Due to chromosome fixation, the relative intensity of selection varied at the same
212 doses of $CuSO_4$ between crosses. Specifically, as shown below, Wine chromosome VIII
213 has a strongly advantageous allele, so the same dose of $CuSO_4$ produces more
214 survivors in the Wine VIII cross than in the Oak VIII cross. We therefore tested multiple
215 doses of $CuSO_4$ to determine the dose that produced 1–10% survival of the population.
216 This range of selection optimizes BSA by balancing detectable effects and retention of
217 causative genetic variation in the surviving population [33]. Unselected bulks from each
218 cross were seeded in YPD at 10% the cell number at which selected bulks were seeded
219 so that their final cell densities were approximately the same as those in the selected
220 bulks.
221

222 Known drivers of resistance are identified as additive QTL

223 Previous studies have identified additive QTL for the trait of copper sulfate
224 resistance in a variety of *S. cerevisiae* strains [2,4,18,34]. In addition, multiple studies
225 have identified mechanistic drivers of copper resistance, including certain alleles of the
226 *FRE1* gene and copy number amplification of the *CUP1* locus [27,35,36]. Because there

227 is overlap across strains for identification of some QTL [37], one form of validation of
228 epic-QTL would be for previously known resistance loci to be detected by epic-QTL as
229 additive effects (that is, effects that do not depend on the parental origin of the fixed
230 chromosome).

231 In epic-QTL, as in standard BSA, allele frequency differences between bulks at a
232 given genomic site indicate a contribution of variation at that site to bulk membership.
233 For the reciprocal chromosome I crosses and, separately, for the reciprocal
234 chromosome VIII crosses, we sequenced the four bulks (selected vs. unselected for
235 each Oak or Wine fixed chromosome) at high depth of coverage (average ~70X per site
236 per bulk) to estimate allele frequencies. We partitioned the effects of selection, parental-
237 chromosome background (hereafter "background"), and their interaction using a logistic
238 regression model as described in *Materials and Methods*. The selection term's
239 coefficient reflects the additive effect on $CuSO_4$ survival regardless of parental-
240 chromosome background, whereas the interaction term reflects epistasis with the fixed
241 chromosome. To visualize significant effects across the genome, we use the z-score of
242 each coefficient. The z-score is advantageous over the parametric *p*-value to which it
243 corresponds because its sign indicates the direction of effect of the fixed chromosome,
244 and because we use permutations of it to determine a threshold of false discovery rate,
245 detailed in *Materials and Methods*. To compare significance regardless of effect
246 direction, the majority of plots display absolute values of z-scores. Signed z-scores for
247 each coefficient and position are included in supplemental data (S1 Table).

248 The additive (selection) peaks on chromosomes VIII and XII are very close to the
249 known copper-resistance genes, *CUP1* and *FRE1*, respectively (Fig 2). These genes

250 are well documented to play critical roles in copper detoxification mechanisms in yeast.
251 *CUP1* encodes a metallothionein involved in sequestering copper ions, thereby
252 mitigating copper toxicity within the cell [38]. *FRE1* encodes a ferric reductase enzyme
253 that contributes to iron uptake and detoxification of copper [39,40]. In both fixed-
254 chromosome backgrounds, we identify *FRE1* as a major driver of resistance, with peak
255 maxima <6 kb away from the coding region (Fig 2). The crosses for the two fixed-
256 chromosome backgrounds are independent, so the agreement between the two crosses
257 further validates the method. In the strains fixed for chromosome I, the peak on
258 chromosome VIII is upstream of the *CUP1* coding sequence. *CUP1* has two paralogs,
259 *CUP1-1* and *CUP1-2*, within a larger tandemly duplicated region in the reference
260 genome of the laboratory strain S288C. We found that the region surrounding these
261 paralogs had poor mapping quality, likely due to repetitive sequences and potential
262 *CUP1* copy variation, which is a known mechanism of resistance [38]. These regions
263 were therefore excluded from our variant calling, and so the peak upstream of the
264 coding sequence is as close as can be to this known driver of copper resistance.
265
266 **Fig 2. Known drivers of copper resistance identified as additive QTL**. Traces
267 represent absolute z-scores of additive (selection) coefficients on chromosomes VIII
268 and XII, as indicated. Dashed line corresponds to the experiment with chromosome I
269 fixed and solid line corresponds to the experiment with chromosome VIII fixed.
270 Horizontal lines indicate the 5% false discovery rate (FDR) threshold for each
271 experiment. Turquoise vertical lines represent the locations of CUP1 and FRE1, both of
272 which fall under large-effect additive peaks as expected.

Fixing Large Effect QTL Increases Power for Detection of Additive Effects

The resolution and reproducibility of epic-QTL are further supported by additive QTL that do not map to known copper-resistance loci. Between the experiment with fixed chromosome I and the experiment with fixed chromosome VIII, we identified many overlapping selection-QTL peaks with locations of highest absolute z-scores within 1.5 kb of one another, indicating not only that there is high resolution and reproducibility but also that the underlying mechanisms of resistance do not strongly differ in the presence of one or the other fixed chromosome (Fig 3, S2 Table).

Fig 3. Consistent additive peaks identified in each fixed parental-chromosome experiment. Additive effects for the experiment with chromosome I fixed (dashed lines) and the experiment with chromosome VIII fixed (solid lines), shown as the absolute value of the selection coefficient's z-score, with 5% FDR thresholds shown as horizontal lines of the same type. The only trace for chromosome I is solid, and the only trace for chromosome VIII is dashed, because of the fixed chromosome in each experiment. Peaks for each experiment are denoted as points on the traces as well as vertical lines below (fixed chromosome I as light blue, top strip, and fixed chromosome VIII as dark blue, bottom strip). In these strips, regions of significant z-scores are shown in gray, with intensities proportional to absolute z-score.

295 Having established that our method identifies additive QTL, we next investigated
296 the result of chromosome fixation on additive effects. Removal of a major-effect QTL is
297 expected to increase the power to detect QTL of lesser effect [41], so we investigated
298 whether epic-QTL has an added benefit of increasing power when a major-effect QTL
299 exists on a fixed chromosome. We found that indeed the majority of peaks in the fixed
300 chromosome VIII experiment had z-scores of greater magnitude than the corresponding
301 peaks in the fixed chromosome I experiment, and that several additional peaks were
302 detected that were not called when chromosome I was fixed (Fig 3). On chromosome
303 XII in particular, only a single peak is obvious in the fixed chromosome I experiment,
304 whereas in the fixed chromosome VIII experiment, two peaks can clearly be
305 differentiated (Fig 3). Taken together, our results for additive QTL demonstrate that
306 epic-QTL has high power, resolution and reproducibility; that copper resistance in the
307 Oak X Wine cross progeny shares at least some underlying mechanisms with other *S.*
308 *cerevisiae* strains; and that removal of a major source of variance can increase power to
309 detect other additive QTL.
310

311 Magnitude epistasis is identified with chromosome VIII but
312 not chromosome I

313 Reciprocal chromosome fixation effectively converts effects that are epistatic with
314 that chromosome into additive effects that can be detected with high power by BSA. In
315 the context of the epic-QTL logistic-regression model, these epistatic effects are
316 identified as significant selection-by-background interactions.

317 We identify seven interactions with chromosome VIII: one each on chromosomes
318 VII, X, XII, XIV, and XV, and two on chromosome XI (Fig 4, S3 Table). The z-score of
319 each interaction peak is less extreme than that of its corresponding additive effect, but
320 not always in the same direction as the additive effect, indicating that there is no
321 consistent interaction effect (such as the Oak chromosome always amplifying Oak
322 alleles' selection effects). We did not identify any interactions at a 5% FDR with
323 chromosome I (Fig 4A), despite observing >10 additive QTL. As chromosome I is the
324 smallest of the *S cerevisiae* chromosomes, it is plausible that there would not be any
325 interactions with the entire chromosome. This result provides evidence that epic-QTL
326 does not generate spurious interactions, and that interactions are specific and not
327 widespread across the genome.
328
329 **Fig 4. Interaction effects indicate magnitude epistasis.** (A) Fixed chromosome I
330 (top) and fixed chromosome VIII (bottom) absolute z-scores for $CuSO_4$ experiments,
331 with trace colors indicating additive (black) and interaction (red) effects.Vertical red lines
332 indicate where an interaction peak has been called, with solid lines indicating the
333 highest peak on a chromosome and dashed lines indicating a second significant peak.
334 (B) Allele frequencies of the Wine allele at the maximum point of each interaction QTL
335 per chromosome (indicated by solid lines in 4A and triangles in 4C), in each population.
336 Oak (O) and Wine (W) fixed chromosome VIII backgrounds are on the horizontal axis,
337 and the allele frequency of the Wine allele is on the vertical axis. Line crossing of
338 selected (blue) and non-selected (gray) would indicate sign epistasis. (C) Comparisons

339 of z-scores at interaction peaks (red triangles) with z-scores at corresponding additive
340 peaks (black triangles).

341 The presence of an interaction can indicate different forms of epistasis. One
342 possibility is sign epistasis, which in the case of epic-QTL would mean that changing the
343 parent of the fixed chromosome changes the direction of the QTL effect at the
344 interacting locus. An alternative possibility is magnitude epistasis, in which the QTL
345 effect size at the interacting locus changes but the direction of the effect remains the
346 same. In experimental designs such as standard BSA, where effects at any locus are
347 averaged across a population, sign epistasis obscures phenotypic effect as the effects
348 of allele pairs cancel each other out. Perfect sign epistasis, in which effect magnitude is
349 equal but effect direction is opposite, is therefore impossible to detect by BSA without
350 fixation of one allele in the pair to isolate the effect. In contrast, magnitude epistasis still
351 produces an additive effect, although the effect size will be the average of that of each
352 allele combination. To characterize our interaction QTL as exhibiting sign or magnitude
353 epistasis with the fixed chromosome, we: 1) compared the allele frequencies of the
354 highest points of the interaction peak (Fig 4C), and 2) scanned for loci above the 5%
355 FDR threshold where the interaction z-score was more extreme than its corresponding
356 additive z-score. Sign epistasis would require line-crossing of allele frequencies
357 between parental backgrounds in the selected bulks, which we do not observe at
358 interaction peaks (Fig 4B). We also do not find any significant interaction z-scores that
359 are greater in magnitude than their selection effect (Fig 4C), which would indicate that
360 the interaction obscures the additive effect through averaging. We therefore conclude
361 that epistasis with chromosome VIII is magnitude and not sign epistasis.

362 Prior studies have identified interaction QTL for copper resistance in *S.*
363 *cerevisiae* either by testing for interactions between additive QTL [4] or by barcoding
364 combinations of alleles in natural variants [21,22]. We compared interactions identified
365 with chromosome VIII in our study with those identified in these other studies, which
366 utilized strains other than the Oak and Wine strains used here. We find that there is little
367 overlap between identified loci (S2 Fig). There are, however, consistent additive effects
368 at specific loci such as *CUP1*, and indeed most interactions with chromosome VIII from
369 the other studies did involve the *CUP1* locus. These results suggest that interactions
370 are between specific alleles not necessarily present in all crosses, which could be
371 corroborated with additional epic-QTL experiments with different parental strains.
372 Further evidence that interaction effects are idiosyncratic is that not every
373 additive locus interacts with the fixed chromosome, and there is no correlation in the
374 direction or magnitude of effect of the interaction compared to additive effect (Fig 4C).
375 The majority of interaction peaks (4 of 7) were within 6 kb of the additive peak maxima,
376 indicating that the interactions with chromosome VIII are likely with the same loci that
377 produce additive effects. Of the remaining interaction peaks, two (the one on
378 chromosome VII and the lesser one on XI) overlap with what appear as shoulders of
379 additive peaks, suggesting that multiple QTL occur within that peak, and that the second
380 largest is interacting with chromosome VIII. The peak on chromosome XV might also
381 correspond more with the shoulder of the additive peak. The interaction peak and
382 corresponding additive peak shoulder on chromosome VII are close to the *CUP2* gene,
383 which induces transcription of *CUP1* [35]. *CUP2* could thus be a candidate for allele
384 substitution to confirm the interaction with *CUP1* on chromosome VIII. Overall, the co-

occurrences of interaction peaks with additive peaks indicate that interactions occur primarily with loci that have an additive effect, and the lack of interactions at every additive peak, or even the most significant additive peaks, suggests that interactions are specific and idiosyncratic.

Discussion

Identifying epistatic contributions to trait variation presents challenges caused by the combinatorial nature of interactions and their potential to obscure effects of individual alleles. Methods to detect pairwise interaction effects suffer from low statistical power due to the number of pairwise comparisons across the genome to test. High power can be achieved by BSA experiments, but averaging over combinations of alleles precludes analysis of interactions. Because of these challenges, approaches to predicting the effect of genotype often minimize the contribution of epistasis to phenotypic variance, by first (or only) fitting additive effects [9]. However, although the effects of epistasis might be statistically underestimated, specific examples of epistasis have been observed across species and traits such as in tomato size and fruit number [42,43], corn kernel coloration [44], and mouse coat color (39, reviewed by 12). In non-natural variants such as deletion mutations or engineered hypomorphs, interactions have also been quantified; using high-throughput approaches, Costanzo *et.al.* found ~900,000 interactions among 23 million double mutants representing nearly every pair of genes in the yeast genome [24], and Hale *et al.* found that over one quarter of 1721 CRISPR-interference perturbations showed growth effects that depend on genetic

407 background [46]. We developed epic-QTL with the aim of bringing the power of a high-
408 throughput, DNA sequencing-based approach to the identification of interactions
409 between natural genetic variants. Specifically, we circumvented the statistical problem
410 of pairwise testing of natural variants by reciprocally fixing a single chromosome from
411 each of two genetic backgrounds in a cross between divergent yeast strains. With the
412 high power afforded by BSA, we observe magnitude epistasis with additive QTL but no
413 evidence of cryptic sign epistasis.

414 We first verified our method by comparing additive QTL identified by epic-QTL,
415 both between experiments with chromosome I or chromosome VIII fixed and between
416 our study and those conducted on copper resistance in other strains. Known drivers of
417 copper resistance, *CUP1* and *FRE1*, were identified as additive QTL in all experiments
418 where the loci were allowed to segregate. Additive peaks colocalized between the
419 experiment with chromosome I fixed and the experiment with chromosome VIII fixed,
420 but on average those identified in the experiment with fixed chromosome VIII were
421 stronger, very likely due to the fixation of a major QTL. In comparison with other studies
422 of copper sulfate resistance, several additive QTL were found in common, but many
423 were not, suggesting strain-specific differences in which alleles are present that impact
424 resistance.

425 The key strength of epic-QTL is identification of interactions with fixed
426 chromosomes at high statistical power. We next compared interactions found by epic-
427 QTL to those identified for copper resistance using different strains, different methods
428 and smaller sample sizes [2,19,21,22], finding that although there is some overlap in
429 regions containing additive QTL, the majority of interactions are not common between

430 studies. This finding speaks to the importance of more high-powered studies of
431 interactions and potentially also suggests that interactions are idiosyncratic in that they
432 are dependent on the specific alleles found in divergent strains. Because we detected
433 more additive than interaction QTL, not every detected additive QTL in our study
434 contained interaction QTL. Moreover, interactions did not necessarily cluster only under
435 the highest additive peaks. This finding further supports that the interactions are
436 idiosyncratic, rather than globally caused by nonlinear transformation of the value of a
437 latent trait with additive genetic architecture [14]. One key overlap with another study to
438 note, however, is *CUP1* as a hub for interactions on chromosome VIII [22]. That
439 interactions occur with chromosome VIII but not chromosome I, and that interactions
440 occur primarily with additive QTL, suggests that our interactions might be with *CUP1*.
441 The logical next step would be to fix the chromosomes found to interact with fixed
442 chromosome VIII, allowing chromosome VIII to segregate, and thereby to identify the
443 interaction partner(s) on this chromosome.
444 The interaction QTL identified here provide evidence of three compelling trends
445 that imply a middle ground between completely idiosyncratic epistasis and highly
446 predictable global epistasis: 1) interaction peaks commonly colocalized with additive
447 peaks, 2) magnitude epistasis was observed whereas sign epistasis was notably
448 absent, and 3) interaction peaks differ between studies and are not driven by strength of
449 an additive peak. Sign epistasis has the potential to completely obscure additive effects,
450 and thus the lack of sign epistasis implies that interactions occur primarily with loci that
451 already have an effect. Precise colocalization of additive and interaction maxima
452 suggest that the additive QTL interacts with the fixed chromosome. These trends

453 corroborate the conclusion by Bloom *et al.* [4] that interactions occur primarily between
454 additive QTL, and they validate the approach of reducing the search space by only
455 looking at interactions between additive QTL as done by Nguyen Ba *et al.* [21].

456 Sign but not magnitude epistasis can influence available evolutionary trajectories
457 by creating valleys between peaks on a fitness landscape [11,13]. Examples of specific
458 reciprocal sign epistasis, for example mutually exclusive adaptive mutations in the
459 *HXT6/7* and *MTH1* genes during experimental evolution under glucose limitation, have
460 been shown to cause fitness valleys [47]. Sign epistasis involving mutations in specific
461 interaction hubs has also been observed [25], but the general prevalence of sign
462 epistasis is yet to be determined. epic-QTL offers an unbiased, powerful method for
463 detecting sign epistasis. The lack of sign epistasis detected here therefore indicates that
464 it is relatively rare, at least for the trait, fixed chromosomes, and parental strains we
465 studied.

466 It will be important to see whether the trends we observed generalize to other
467 fixed chromosomes and other complex traits. A complete set of fixed-chromosome
468 strains would yield an additional benefit of very rapid assessment of the extent to which
469 epistasis impacts variation in a trait, in that a completely additive genetic architecture
470 would mean that the sum of chromosome effects should equal the difference between
471 the parental strains. Such a test only requires chromosome-substituted strains, not
472 segregants from them. When this kind of test was applied in mice and rats to a large
473 number of anatomical and physiological traits, it revealed much evidence for epistasis
474 [48].

475 A widespread lack of sign epistasis would greatly aid in identifying interactions in
476 studies where experimental manipulations of genotypes are not possible. Genome-wide
477 association studies in particular face challenges with respect to the number of subjects
478 relative to the number of possible interactions between markers, and so a variety of
479 methods have been proposed to avoid exhaustively searching all possible pairs of
480 polymorphisms [49]. Prioritizing interactions between additive loci rather than every
481 possible combination could therefore be a principled approach to increase the power to
482 detect interaction effects. Characterizing interaction effects in humans should in turn
483 allow for greater precision in predicting response to medication and susceptibility to
484 disease, as well as facilitate further understanding of the molecular mechanisms of
485 complex traits. In all, our characterization of epistasis not only enhances our
486 understanding of genetic interactions in model organisms but also has implications for
487 improvement of applications in personalized medicine and trait prediction across diverse
488 species.
489

490 # Materials and Methods

491 ## Conditional Chromosome Strain Construction

492 Two divergent haploid yeast strains, one oak tree-derived (NCYC3631, MATα)
493 and one wine barrel-derived (NCYC3591, MATa) [29], were each engineered for
494 chromosome removal from diploids and later selection of haploid progeny. To facilitate
495 crosses, strains were modified by homologous recombination at *URA3*, *HO*, and *MAT*α
496 using standard lithium-acetate-based transformation. *URA3* prototrophy was restored
497 (and *KanMX* removed) in wine-derived strains by insertion of *URA3* sequence amplified

498 from the wine-strain parent (BC187). The positive-selection marker *hph*, which confers
499 resistance to hygromycin, was removed from the *HO* locus of each parental strain to
500 allow the marker's use elsewhere. To remove *hph*, we conducted Delitto Perfetto
501 excision [50] using a cassette that allows positive selection for nourseothricin resistance
502 (*NatR*) and negative selection against HSV-*TK*, which encodes the thymidine kinase
503 from herpes simplex virus and thereby confers sensitivity to the pyrimidine analogue 5-
504 fluorodeoxyuridine (FuDR) [51]. Importantly, two identical sequences (*cyc* terminators)
505 flank this cassette and thereby lead to spontaneous excision of the cassette by
506 homology-based repair [50]. Transformants were selected for presence of *NatR* and
507 checked for loss of *hph*. We then counter-selected using FuDR to select for removal of
508 the cassette and resulting loss of both *NatR* and HSV-*TK*.
509 To select for haploids of one mating type in bulks to be sequenced, we
510 engineered the *MATα* locus to contain the HSV-*TK* negative-selection marker for
511 removal of any cell that is not a mating-type a haploid. *MATα* contains a bidirectional
512 promoter driving the expression of the *α1* and *α2* genes, both of which must be active
513 for the cell to sporulate [52]. The negative-selection marker was inserted upstream of *α1*
514 and its promoter, and the *STE3* promoter (*pSTE3*), which is activated by the
515 transcriptional co-activator encoded by *α1*, was placed upstream of *α2* [53]. Thus, the
516 selection cassette was placed in a way that maintains expression of both *α1* and *α2* in
517 mating-type α haploids and in diploids. As a result, the cells retain the ability to mate
518 with mating-type a cells as haploids and to sporulate as diploids, but both diploids and
519 haploid mating-type α haploids are sensitive to FuDR. For this transformation we used
520 the positive-selection marker *hph*. We transformed a cassette containing MATα

521 homology and the positive- and negative-selection markers into the Oak α strain, and
522 then replaced *hph* with *NatR* using lithium acetate homology-directed transformation,
523 allowing use of *hph* in later transformations.

524 For chromosome elimination by driving transcription through the centromere, we
525 constructed an inducible-promoter cassette by using overlapping PCR to combine the
526 HSV-*TK* and *hph* markers from Alexander *et al.* [51], the *GAL1* promoter (*pGAL1*), and
527 regions homologous to the yeast genome adjacent to the centromere. The centromere-
528 region primers matched the primers used by Reid *et al.* [30] or matched sequences very
529 close nearby. These cassettes were transformed into either chromosome I or
530 chromosome VIII in either the Oak α or Wine *a* strains. All strains are detailed in
531 supplemental data (S4 Table). These haploid strains are referred to as the background
532 (Wine a or Oak α) plus [I] or [VIII] to indicate the chromosome that can be eliminated.

533 Wine a[I] and Oak α were mated to produce diploids, and Wine a and Oak α[I]
534 were mated to produce diploids capable of producing the reciprocal chromosome
535 fixation (Fig 1A). Diploids were selected by ability to grow in both the absence of uracil
536 and the presence of nourseothricin, and ploidy was confirmed by flow cytometry using
537 DNA staining with propidium iodide on the Cytek Aurora. To fix chromosome I, diploids
538 were then plated onto medium containing 2% D-Galactose (and lacking glucose) to
539 induce the *GAL1* promoter's transcription through the centromere of the conditional
540 chromosome. Although we did not use markers to select for the loss of a chromosome,
541 plating on galactose and restreaking from single colonies was effective for yielding
542 chromosome loss. Colonies from the restreaked plate were checked by Sanger
543 sequencing to identify a loss of the conditional chromosome (i.e. by loss of

544 heterozygosity on that chromosome), then grown in liquid media and frozen as clonal
545 aneuploid (2N–1) strains, which we term Oak I or Wine I to indicate the parent of origin
546 of the remaining chromosome I in these otherwise hybrid strains. Populations of ~10^7
547 clonal aneuploids were sporulated using 2% potassium acetate for ~10 days at room
548 temperature (25 °C) to produce approximately $4X10^7$ segregants with identical
549 chromosome I of either Oak or Wine background but segregating parental genotypes at
550 all other loci. To select for haploids above and beyond the MAT*α* selection, spores were
551 vortexed for 10 minutes in 50% diethyl ether to kill unsporulated diploids [54]. Surviving
552 spores were rinsed twice in sterile water, then germinated by incubation in 1 mg/mL
553 Zymolyase (Z100T) for 12 minutes before culturing in each experiment. The process
554 was completed identically for the reciprocal fixations of chromosome VIII.
555

556 ## Concentration Determination for Selection

557 We tested approximate concentrations of copper for selection by growing cells in
558 media of different concentrations for 24 hours (matching the experiment time) and then
559 counting the cells either by automatic cell counter (ThermoFisher Countess™ II) or by
560 manual counting on a hemocytometer. From there, we chose smaller ranges of doses
561 that would provide between 1% and 10% survival. After conducting experiments, cell
562 counts in some experiments were checked by hemocytometer to confirm that
563 experimental treatments were achieving the intended amount of selection.
564

565 ## Bulk Segregant Analysis

566 Pools of segregants with reciprocal fixed chromosomes (Oak I and Wine I, or
567 Oak VIII and Wine VIII) were grown in parallel for 24 hours in either YPD or YPD +
568 copper sulfate at doses determined in each chromosome-fixed bulk population to
569 produce between 1% and 10% survival. The control cultures grown in YPD were
570 seeded at 10% of the starting density for the selected group. Each of the four bulk
571 categories was grown in duplicate. After 24 hours, each of these bulks was harvested
572 by spinning down cells separately and extracting DNA either by phenol-chloroform-
573 isoamyl alcohol extraction and ethanol precipitation [55], or by Qiagen DNeasy Blood
574 and Tissue Extraction Kit 69506.

575

576 ## Sequencing

577 After DNA was harvested, single-end libraries for DNA sequencing were
578 prepared according to Baym *et al.*'s protocol [56] using Illumina kit FC-131-2001 and
579 KAPA HiFi amplification kit KK2612. Fragments were selected to be 200–600 bp by
580 AMPure XP bead cleanup (Fisher NC9959336), and pooled based on concentrations
581 determined by LifeTechnologies Qubit 3.0 and Roche 480 LightCycler qPCR. Libraries
582 were then sequenced on an Illumina NovaSeq 6000, with an average per-bulk depth of
583 ~70X. Reads were aligned to the S288C reference genome R64 using BWA-MEM [57],
584 sorted using PicardTools [58], and then underwent quality control using Genome
585 Analysis Toolkit [59] command *BQSR*. Variants were called using GATK
586 *HaplotypeCaller* [60] as described by Mansfield and Grumet [61].

587

588 ## epic-QTL Analysis

589 VCFs were converted to tables of reads to analyze in R using GATK's
590 *VariantsToTable* function. We first removed all loci with >2 alternate alleles to control for
591 mapping quality issues, then assigned each alternate allele to the corresponding parent
592 based on SNP location from whole genome sequencing of the parent strains [62]. To
593 increase our signal-to-noise ratio and take advantage of the inherent correlation of
594 nearby genomic positions in a single F2 cross, we smoothed the read counts in rolling
595 windows of 200 SNPs using a Gaussian weighted mean.

596 To partition the effects of fixed-chromosome parent of origin, selection, and their
597 interaction, we performed logistic regression on these counts for each smoothed
598 position using the following formula:

599

600 $$\log(\textit{allele odds}) = \beta 0 + \beta 1 \cdot \textit{selection} + \beta 2 \cdot \textit{background} + \beta 3 \cdot (\textit{selection} \times \textit{background}) + \epsilon$$

601

602 where *selection* is the presence or absence of copper sulfate in the culture media,
603 *background* is the parent of origin of the fixed chromosome, and the
604 *selection×background* term captures the dependence on background of the selection
605 effect, i.e. epistasis. We then used the z-scores of each effect to identify additive
606 (*selection*) and epistatic (*selection×background*) QTL. Absent any effects of the fixed
607 chromosome's parent of origin on segregation of the other chromosomes or on growth
608 in the absence of copper sulfate, we do not expect to see a significant background
609 effect. For this reason, we set the contrasts of the selection variable to 0 (copper

610 absent) and 1 (copper present), and for the background variable to –0.5 (Wine) and 0.5
611 (Oak). Outputs of this analysis are available in supplemental data (S1 Table).
612 To establish our statistical threshold for interactions, we conducted permutations
613 of allele frequency ratios by shuffling positions within each parent and replicate in the
614 non-selected bulks. This permutation approach is based on the assumption that, in the
615 absence of selection, there would be no loci associated with the trait. For the
616 permutations, we excluded chromosomes I and VIII from all experiments to remove the
617 effect of the fixed chromosomes, and removed chromosomes III and V, which contained
618 engineered regions not identical in the two parents. We then assigned bulks randomly
619 to these permuted values according to the structure of the original dataset (the same
620 number of replicates in each group) and calculated our selection, background, and
621 interaction effects for each. These effects drawn from the bulks of two different parents
622 form the null distribution of z-scores of interaction effects for each experiment. All
623 analyses employ a false discovery rate threshold of 5%.
624 Peaks of absolute z-score (QTL locations) were called by identifying the
625 maximum points within chromosome segments bounded by chromosome ends or local
626 minima, defined as positions where the local slope of the absolute z-score trace shifted
627 from negative to positive. The local slope was calculated within sliding windows of 700
628 SNPs by linear regression within the window. The highest point in that segment, if
629 above the 5% FDR, was then called as the peak. Additive and interaction peak locations
630 are available in supplemental data (S2 and S3 Tables).

631

632 # Acknowledgements

633 This work was supported in part through the NYU IT High Performance Computing
634 resources, services, and staff expertise. We acknowledge the Zegar Family Foundation
635 for their generous support. We thank the NYU Center for Genomics and System Biology
636 Genomics Core for their assistance and resources. We thank members and alumni of
637 the Siegal lab for input on the paper and discussion about the project.

638

639 # References

640 1. Tsouris A, Fournier T, Friedrich A, Hou J, Dunham MJ, Schacherer J. Species-wide survey
641 of the expressivity and complexity spectrum of traits in yeast. PLOS Genet. 2024;20:
642 e1011119. doi:10.1371/journal.pgen.1011119
643 2. Bloom JS, Ehrenreich IM, Loo WT, Lite T-LV, Kruglyak L. Finding the sources of missing
644 heritability in a yeast cross. Nature. 2013;494: 234–237. doi:10.1038/nature11867
645 3. Mackay TFC, Stone EA, Ayroles JF. The genetics of quantitative traits: challenges and
646 prospects. Nat Rev Genet. 2009;10: 565–577. doi:10.1038/nrg2612
647 4. Bloom JS, Kotenko I, Sadhu MJ, Treusch S, Albert FW, Kruglyak L. Genetic interactions
648 contribute less than additive effects to quantitative trait variation in yeast. Nat Commun.
649 2015;6: 8712. doi:10.1038/ncomms9712
650 5. Falconer D, Mackay TFC. Introduction to Quantitative Genetics. IV. Longman Group Ltd;
651 1996.
652 6. Lynch M, Walsh B. Genetics and Analysis of Quantitative Traits. Sinauer Associates, Inc;
653 7. Boye C, Nirmalan S, Ranjbaran A, Luca F. Genotype × environment interactions in gene
654 regulation and complex traits. Nat Genet. 2024;56: 1057–1068. doi:10.1038/s41588-024-

01776-w

8. Morgante F, Huang W, Maltecca C, Mackay TFC. Effect of genetic architecture on the prediction accuracy of quantitative traits in samples of unrelated individuals. Heredity. 2018;120: 500–514. doi:10.1038/s41437-017-0043-0

9. Ober U, Huang W, Magwire M, Schlather M, Simianer H, Mackay TFC. Accounting for Genetic Architecture Improves Sequence Based Genomic Prediction for a Drosophila Fitness Trait. 2015. doi:doi.org/10.1371/journal.pone.0126880

10. Mackay TFC, Anholt RRH. Pleiotropy, epistasis and the genetic architecture of quantitative traits. Nat Rev Genet. 2024;25: 639–657. doi:10.1038/s41576-024-00711-3

11. Weinreich DM, Watson RA, Chao L. Perspective: Sign epistasis and genetic constraint on evolutionary trajectories. Evol Int J Org Evol. 2005;59: 1165–1174.

12. Phillips PC. Epistasis—the essential role of gene interactions in the structure and evolution of genetic systems. Nat Rev Genet. 2008;9: 855–867. doi:10.1038/nrg2452

13. Phillips PC, Otto SP, Whitlock MC. Beyond the average: the evolutionary importance of gene interactions and variability of epistatic effects. Epistasis and the Evolutionary Process. Oxford; 2000.

14. Otwinowski J, Plotkin JB. Inferring fitness landscapes by regression produces biased estimates of epistasis. Proc Natl Acad Sci. 2014;111: E2301–E2309. doi:10.1073/pnas.1400849111

15. Kryazhimskiy S, Rice DP, Jerison ER, Desai MM. Microbial evolution. Global epistasis makes adaptation predictable despite sequence-level stochasticity. Science. 2014;344: 1519–1522. doi:10.1126/science.1250939

16. Johnson MS, Reddy G, Desai MM. Epistasis and evolution: recent advances and an outlook for prediction. BMC Biol. 2023;21: 120. doi:10.1186/s12915-023-01585-3

17. Reddy G, Desai MM. Global epistasis emerges from a generic model of a complex trait. Barkai N, Petrov DA, Crona K, Krug J, editors. eLife. 2021;10: e64740.

681 doi:10.7554/eLife.64740
682 18. Ehrenreich IM, Torabi N, Jia Y, Kent J, Martis S, Shapiro JA, et al. Dissection of genetically
683 complex traits with extremely large pools of yeast segregants. Nature. 2010;464: 1039–
684 1042. doi:10.1038/nature08923
685 19. Ehrenreich IM, Bloom J, Torabi N, Wang X, Jia Y, Kruglyak L. Genetic architecture of
686 highly complex chemical resistance traits across four yeast strains. PLoS Genet. 2012;8:
687 e1002570. doi:10.1371/journal.pgen.1002570
688 20. Nadeau JH, Singer JB, Matin A, Lander ES. Analysing complex genetic traits with
689 chromosome substitution strains. Nat Genet. 2000;24: 221–225. doi:10.1038/73427
690 21. Nguyen Ba AN, Lawrence KR, Rego-Costa A, Gopalakrishnan S, Temko D, Michor F, et
691 al. Barcoded bulk QTL mapping reveals highly polygenic and epistatic architecture of
692 complex traits in yeast. Verstrepen KJ, Barkai N, Verstrepen KJ, editors. eLife. 2022;11:
693 e73983. doi:10.7554/eLife.73983
694 22. Matsui T, Mullis MN, Roy KR, Hale JJ, Schell R, Levy SF, et al. The interplay of additivity,
695 dominance, and epistasis on fitness in a diploid yeast cross. Nat Commun. 2022;13: 1463.
696 doi:10.1038/s41467-022-29111-z
697 23. Michelmore RW, Paran I, Kesseli RV. Identification of markers linked to disease-resistance
698 genes by bulked segregant analysis: a rapid method to detect markers in specific genomic
699 regions by using segregating populations. Proc Natl Acad Sci U S A. 1991;88: 9828–9832.
700 24. Costanzo M, VanderSluis B, Koch EN, Baryshnikova A, Pons C, Tan G, et al. A global
701 interaction network maps a wiring diagram of cellular function. Science. 2016;353:
702 aaf1420. doi:10.1126/science.aaf1420
703 25. Ang RML, Chen S-AA, Kern AF, Xie Y, Fraser HB. Widespread epistasis among beneficial
704 genetic variants revealed by high-throughput genome editing. Cell Genomics. 2023;3:
705 100260. doi:10.1016/j.xgen.2023.100260
706 26. Rehman M, Liu L, Wang Q, Saleem MH, Bashir S, Ullah S, et al. Copper environmental

707 toxicology, recent advances, and future outlook: a review. Environ Sci Pollut Res. 2019;26:
708 18003–18016. doi:10.1007/s11356-019-05073-6
709 27. De Freitas J, Wintz H, Hyoun Kim J, Poynton H, Fox T, Vulpe C. Yeast, a model organism
710 for iron and copper metabolism studies. Biometals. 2003;16: 185–197.
711 doi:10.1023/A:1020771000746
712 28. Valentine JS, Gralla EB. Delivering Copper Inside Yeast and Human Cells. Science.
713 1997;278: 817–818. doi:10.1126/science.278.5339.817
714 29. Cubillos FA, Louis EJ, Liti G. Generation of a large set of genetically tractable haploid and
715 diploid Saccharomyces strains. FEMS Yeast Res. 2009;9: 1217–1225. doi:10.1111/j.1567-
716 1364.2009.00583.x
717 30. Reid RJD, Sunjevaric I, Voth WP, Ciccone S, Du W, Olsen AE, et al. Chromosome-Scale
718 Genetic Mapping Using a Set of 16 Conditionally Stable Saccharomyces cerevisiae
719 Chromosomes. Genetics. 2008;180: 1799–1808. doi:10.1534/genetics.108.087999
720 31. Clowers KJ, Heilberger J, Piotrowski JS, Will JL, Gasch AP. Ecological and Genetic
721 Barriers Differentiate Natural Populations of Saccharomyces cerevisiae. Mol Biol Evol.
722 2015;32: 2317–2327. doi:10.1093/molbev/msv112
723 32. Gerke JP, Chen CTL, Cohen BA. Natural Isolates of Saccharomyces cerevisiae Display
724 Complex Genetic Variation in Sporulation Efficiency. Genetics. 2006;174: 985–997.
725 doi:10.1534/genetics.106.058453
726 33. Magwene PM, Willis JH, Kelly JK. The Statistics of Bulk Segregant Analysis Using Next
727 Generation Sequencing. PLOS Comput Biol. 2011;7: e1002255.
728 doi:10.1371/journal.pcbi.1002255
729 34. She R, Jarosz DF. Mapping Causal Variants with Single-Nucleotide Resolution Reveals
730 Biochemical Drivers of Phenotypic Change. Cell. 2018;172: 478-490.e15.
731 doi:10.1016/j.cell.2017.12.015
732 35. Welch J, Fogel S, Buchman C, Karin M. The CUP2 gene product regulates the expression

733 of the CUP1 gene, coding for yeast metallothionein. EMBO J. 1989;8: 255–260.
734 36. Jungmann J, Reins HA, Lee J, Romeo A, Hassett R, Kosman D, et al. MAC1, a nuclear
735 regulatory protein related to Cu-dependent transcription factors is involved in Cu/Fe
736 utilization and stress resistance in yeast. EMBO J. 1993;12: 5051–5056.
737 doi:10.1002/j.1460-2075.1993.tb06198.x
738 37. Taylor MB, Ehrenreich IM. Higher-order genetic interactions and their contribution to
739 complex traits. Trends Genet. 2015;31: 34–40. doi:10.1016/j.tig.2014.09.001
740 38. Adamo GM, Lotti M, Tamás MJ, Brocca S. Amplification of the CUP1 gene is associated
741 with evolution of copper tolerance in Saccharomyces cerevisiae. Microbiol Read Engl.
742 2012;158: 2325–2335. doi:10.1099/mic.0.058024-0
743 39. Hassett R, Kosman DJ. Evidence for Cu(II) Reduction as a Component of Copper Uptake
744 by *Saccharomyces cerevisiae*(∗). J Biol Chem. 1995;270: 128–134.
745 doi:10.1074/jbc.270.1.128
746 40. Georgatsou E, Alexandraki D. Regulated expression of the Saccharomyces cerevisiae
747 Fre1p/Fre2p Fe/Cu reductase related genes. Yeast Chichester Engl. 1999;15: 573–584.
748 doi:10.1002/(SICI)1097-0061(199905)15:7<573::AID-YEA404>3.0.CO;2-7
749 41. Sinha H, David L, Pascon RC, Clauder-Münster S, Krishnakumar S, Nguyen M, et al.
750 Sequential Elimination of Major-Effect Contributors Identifies Additional Quantitative Trait
751 Loci Conditioning High-Temperature Growth in Yeast. Genetics. 2008;180: 1661–1670.
752 doi:10.1534/genetics.108.092932
753 42. Eshed Y, Zamir D. Less-than-additive epistatic interactions of quantitative trait loci in
754 tomato. Genetics. 1996;143: 1807–1817. doi:10.1093/genetics/143.4.1807
755 43. Aguirre L, Hendelman A, Hutton SF, McCandlish DM, Lippman ZB. Idiosyncratic and dose-
756 dependent epistasis drives variation in tomato fruit size. Science. 2023;382: 315–320.
757 doi:10.1126/science.adi5222
758 44. Ford RH. Inheritance of Kernel Color in Corn: Explanations & Investigations. Am Biol

759 Teach. 2000;62: 181–188. doi:10.2307/4450870
760 45. Bennett DC, Lamoreux ML. The color loci of mice--a genetic century. Pigment Cell Res.
761 2003;16: 333–344. doi:10.1034/j.1600-0749.2003.00067.x
762 46. Hale JJ, Matsui T, Goldstein I, Mullis MN, Roy KR, Ville CN, et al. Genome-scale analysis
763 of interactions between genetic perturbations and natural variation. Nat Commun. 2024;15:
764 4234. doi:10.1038/s41467-024-48626-1
765 47. Kvitek DJ, Sherlock G. Reciprocal Sign Epistasis between Frequently Experimentally
766 Evolved Adaptive Mutations Causes a Rugged Fitness Landscape. PLOS Genet. 2011;7:
767 e1002056. doi:10.1371/journal.pgen.1002056
768 48. Shao H, Burrage LC, Sinasac DS, Hill AE, Ernest SR, O'Brien W, et al. Genetic
769 architecture of complex traits: Large phenotypic effects and pervasive epistasis. Proc Natl
770 Acad Sci. 2008;105: 19910–19914. doi:10.1073/pnas.0810388105
771 49. Van Steen K, Moore JH. How to increase our belief in discovered statistical interactions via
772 large-scale association studies? Hum Genet. 2019;138: 293–305. doi:10.1007/s00439-
773 019-01987-w
774 50. Storici F, Resnick MA. Delitto PerfettoTargeted Mutagenesis in Yeast with
775 Oligonucleotides. In: Setlow JK, editor. Genetic Engineering. Boston, MA: Springer US;
776 2003. pp. 189–207. doi:10.1007/978-1-4615-0073-5_9
777 51. Alexander WG, Doering DT, Hittinger CT. High-Efficiency Genome Editing and Allele
778 Replacement in Prototrophic and Wild Strains of Saccharomyces. Genetics. 2014;198:
779 859–866. doi:10.1534/genetics.114.170118
780 52. Haber JE. Mating-Type Genes and *MAT* Switching in *Saccharomyces cerevisiae*.
781 Genetics. 2012;191: 33–64. doi:10.1534/genetics.111.134577
782 53. Sprague GF, Jensen R, Herskowitz I. Control of yeast cell type by the mating type locus:
783 positive regulation of the alpha-specific STE3 gene by the MAT alpha 1 product. Cell.
784 1983;32: 409–415. doi:10.1016/0092-8674(83)90460-9

785 54. Dawes IW, Hardie ID. Selective killing of vegetative cells in sporulated yeast cultures by
786 exposure to diethyl ether. Mol Gen Genet MGG. 1974;131: 281–289.
787 doi:10.1007/BF00264859
788 55. Green MR, Sambrook J. Isolation and Quantification of DNA. Cold Spring Harb Protoc.
789 2018;2018. doi:10.1101/pdb.top093336
790 56. Baym M, Kryazhimskiy S, Lieberman TD, Chung H, Desai MM, Kishony R. Inexpensive
791 Multiplexed Library Preparation for Megabase-Sized Genomes. PLOS ONE. 2015;10:
792 e0128036. doi:10.1371/journal.pone.0128036
793 57. Li H, Durbin R. Fast and accurate long-read alignment with Burrows–Wheeler transform.
794 Bioinformatics. 2010;26: 589–595. doi:10.1093/bioinformatics/btp698
795 58. Picard Tools - By Broad Institute. [cited 26 Sep 2024]. Available:
796 http://broadinstitute.github.io/picard/
797 59. Van Der Auwera GA, Carneiro MO, Hartl C, Poplin R, Del Angel G, Levy-Moonshine A, et
798 al. From FastQ Data to High-Confidence Variant Calls: The Genome Analysis Toolkit Best
799 Practices Pipeline. Curr Protoc Bioinforma. 2013;43. doi:10.1002/0471250953.bi1110s43
800 60. Poplin R, Ruano-Rubio V, DePristo MA, Fennell TJ, Carneiro MO, Van Der Auwera GA, et
801 al. Scaling accurate genetic variant discovery to tens of thousands of samples. 2017.
802 doi:10.1101/201178
803 61. Mansfeld BN, Grumet R. QTLseqr: An R Package for Bulk Segregant Analysis with Next-
804 Generation Sequencing. Plant Genome. 2018;11. doi:10.3835/plantgenome2018.01.0006
805 62. Ziv N, Shuster BM, Siegal ML, Gresham D. Resolving the Complex Genetic Basis of
806 Phenotypic Variation and Variability of Cellular Growth. Genetics. 2017;206: 1645–1657.
807 doi:10.1534/genetics.116.195180

808

809 # Supporting information captions

810 **S1 Fig. Survival percentage by strain in CuSO4.** Boxplots of survival percentages of
811 Oak (NCYC3631) and Wine (NCYC3591) haploid strains at different concentrations of
812 copper sulfate are shown. Replicate experiments carried out on different dates are
813 represented by different shapes.

814

815 **S2 Fig. Comparison with copper sulfate interaction peaks from previous studies.**
816 Interactions with chromosome VIII identified in our study (shown in black trace of the
817 absolute z-score by genome position) are compared with interaction QTL involving
818 chromosome VIII identified in other copper-resistance studies, which used both different
819 experimental designs and different strains. Beneath the trace from this study, NB
820 (magenta) indicates interaction QTL as identified by Nguyen Ba et al [21], M (turquoise)
821 represents interaction hotspots between strains from Matsui et al. [22], and B (dark
822 blue) represents interaction QTL as identified by Bloom et al [4]. Red vertical lines
823 indicate significant peaks called in our study. *CUP1* is indicated by the vertical light blue
824 dotted line on Chromosome VIII.

825

826 **S1 Table. Logistic regression output**. Direct output from logistic regression on
827 sequencing data for each divergent SNP that passes quality filters (see github for code).
828 Each row (numbered in column A) records the effect term in the model (Background,
829 Bulk, Interaction, or intercept (column B, “label”); the chromosome fixed in the
830 experiment (column C, “chr”); the chromosome containing the SNP (column D,

831 “CHROM”); the chromosomal position of the SNP (column E, “POS”); the z-score of that
832 SNP in that experiment and for the specified effect (column F, “zscore”); and the
833 threshold value for a 5% FDR for the specified effect and experiment (column G, “q5”).
834
835 **S2 Table. Additive-effect peaks**. Peaks called for the Bulk effect. Each row records
836 the chromosome fixed in the experiment (column A, “CSS”), the location of the peak
837 SNP as its chromosome (column B, “CHROM”) and chromosomal position (column C,
838 “POS”), and the z-score of the peak SNP (column D, “zscore”).
839
840 **S3 Table. Interaction peaks**. Peaks called for the Interaction effect. Columns are as in
841 S2 Table.
842
843 **S4 Table. Yeast strains constructed and used in experiments**. Backgrounds,
844 genotypes, and aliases of all strains used, including those representing intermediate
845 steps to construct strains for epic-QTL experiments. MLS.CB refers to strains made in
846 this study; NCYC refers to strains from the NCYC collection [29].

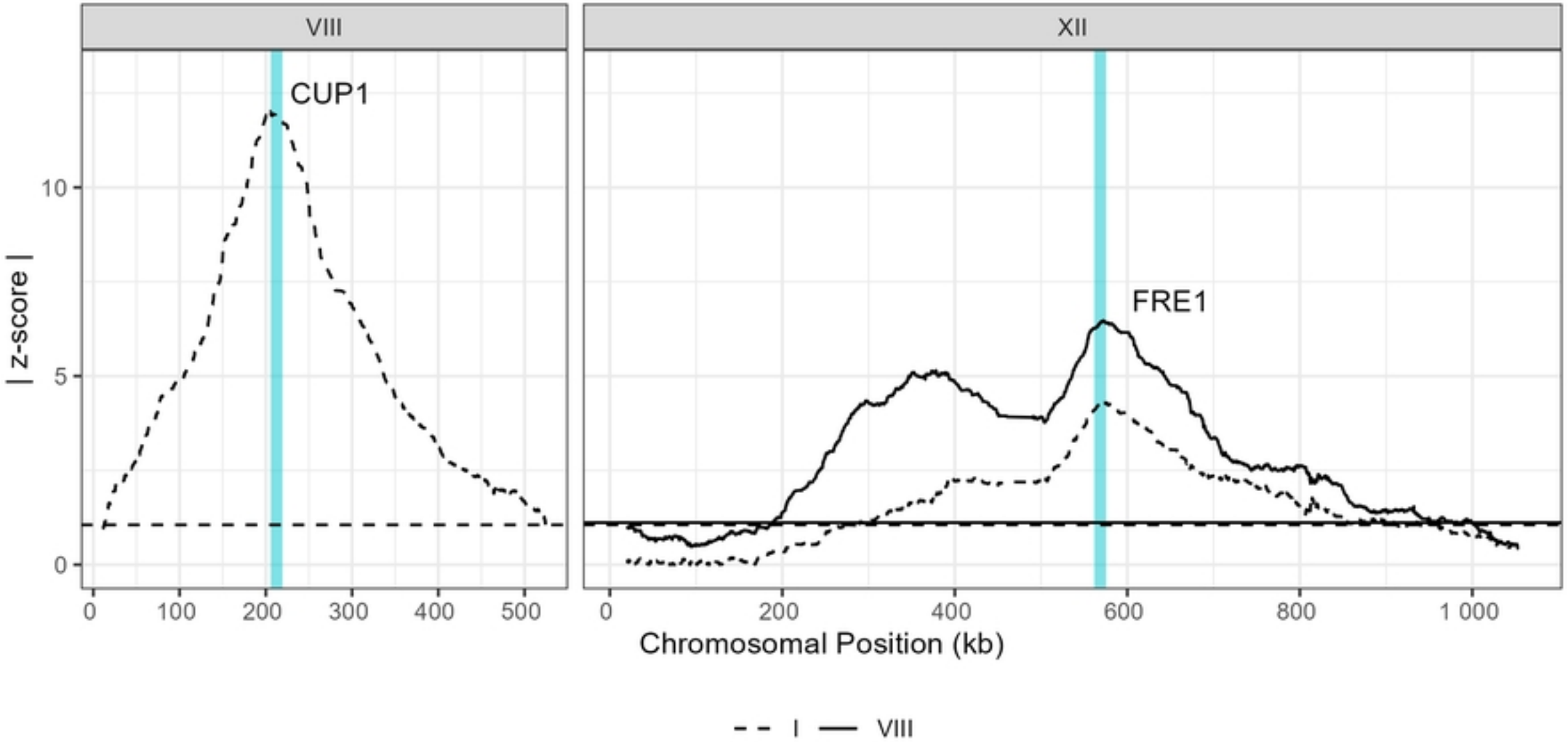
VIII
XII
CUP1
FRE1
| z-score |
10
5
0
0
100
200
300
400
500
0
200
400
600
800
1 000
Chromosomal Position (kb)
I
VIII

Fig 2

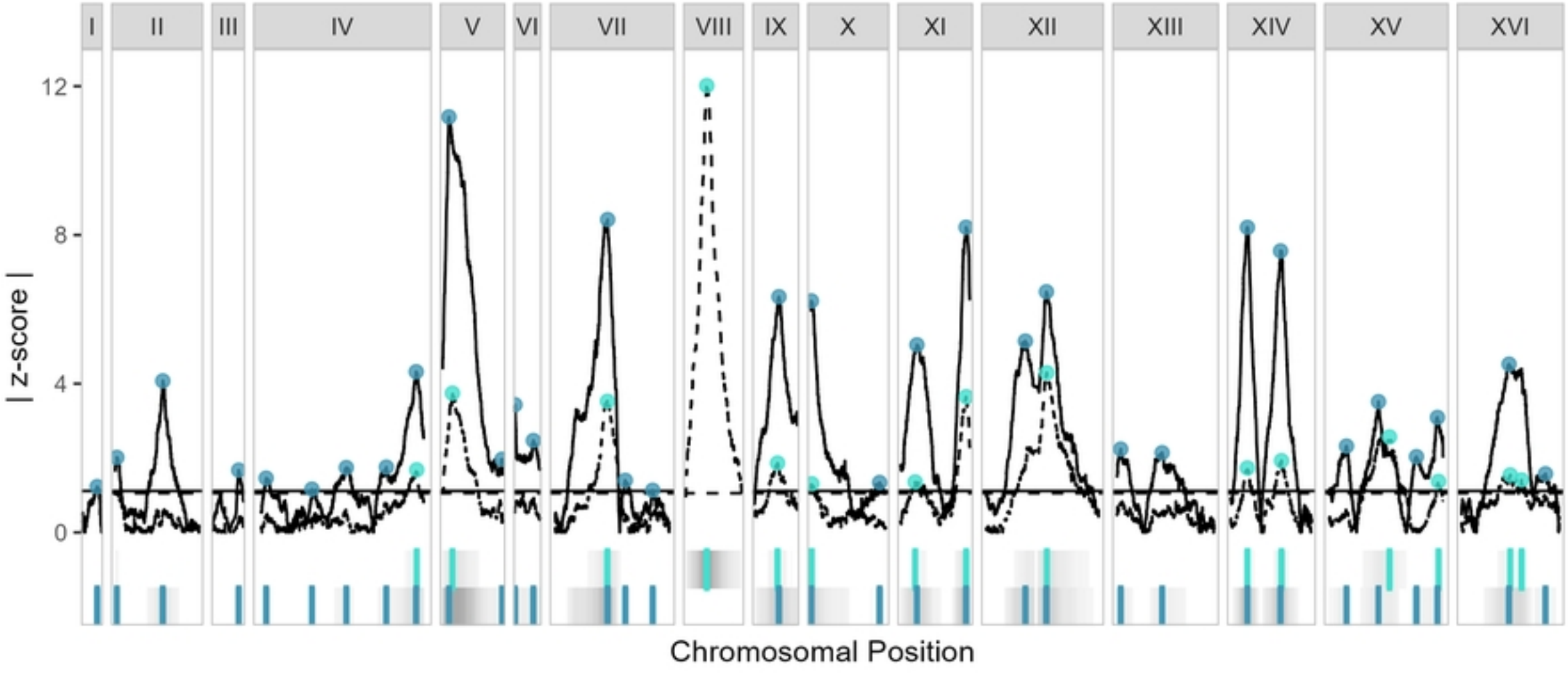
I
II
III
IV
V
VI
VII
VIII
IX
X
XI
XII
XIII
XIV
XV
XVI
12
8
4
0
| z-score |
Chromosomal Position

Fig 3

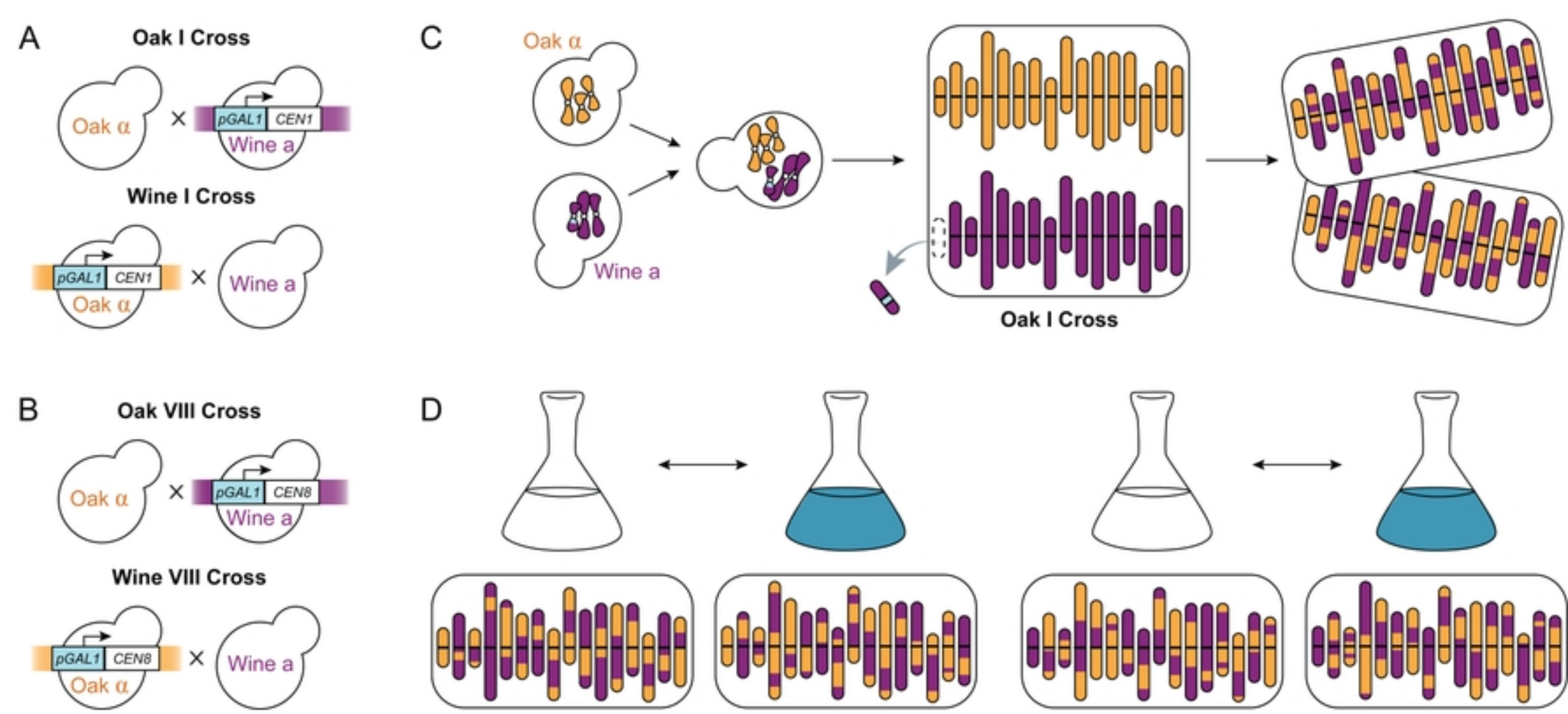
A
Oak I Cross
Oak α
×
pGAL1
CEN1
Wine a
Wine I Cross
pGAL1
CEN1
Oak α
×
Wine a
B
Oak VIII Cross
Oak α
×
pGAL1
CEN8
Wine a
Wine VIII Cross
pGAL1
CEN8
Oak α
×
Wine a
C
Oak α
Wine a
Oak I Cross
D

Fig 1

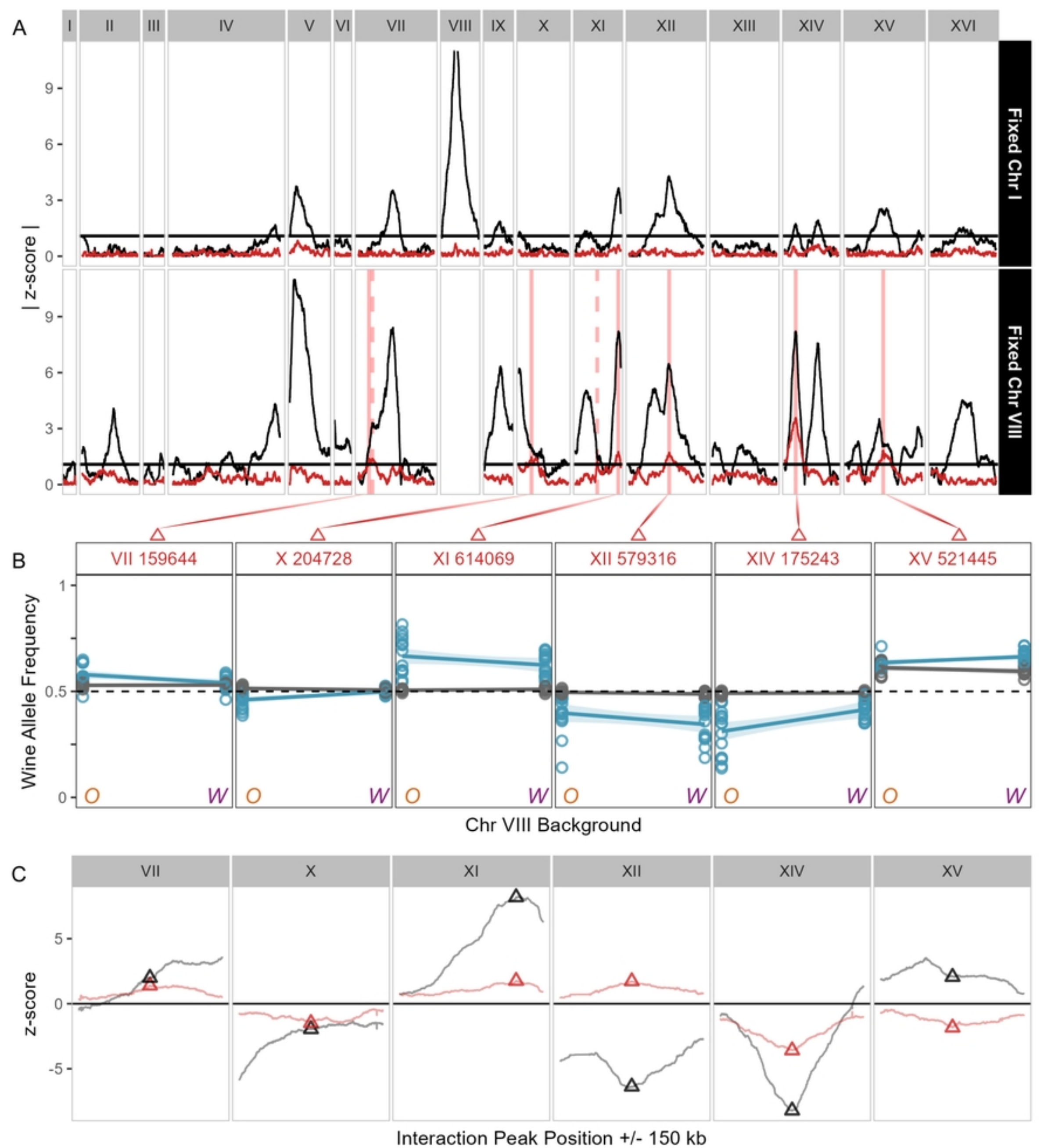
A
I
II
III
IV
V
VI
VII
VIII
IX
X
XI
XII
XIII
XIV
XV
XVI
Fixed Chr I
Fixed Chr VIII
| z-score |
B
VII 159644
X 204728
XI 614069
XII 579316
XIV 175243
XV 521445
Wine Allele Frequency
O
W
Chr VIII Background
C
VII
X
XI
XII
XIV
XV
z-score
Interaction Peak Position +/- 150 kb

Fig 4